*High Temperatures-High Pressures*, Vol. 52, pp. 435–464
Reprints available directly from the publisher
Photocopying permitted by license only
DOI: 10.32908/hthp.v52.1485



# A parameter-free model for temperature and pressure profiles in luminous, stable stars

ANNE M. HOFMEISTER* AND ROBERT E. CRISS

*Department of Earth and Planetary Science, Washington University, St. Louis, MO 63130, USA*

*Received: May 13, 2023; Accepted: July 4, 2023.*

The historic, classical thermodynamic model of star interiors neglects luminosity ($L$), and consequently predicts ultrahigh central solar temperatures ($T \sim 15 \times 10^6$ K). Modern models yield similar $T$ profiles mostly because local thermal equilibrium and multiple free parameters are used. Instead, long-term stability of stars signifies disequilibrium where energy generated equals energy emitted. We assume that heat is generated in a shell defining the core and use Fourier's model, which describes diffusion of heat, including via radiation, to predict the $T$ profile. Under steady-state, power $L$ transmitted through each shell is constant above the zone of energy generation. Hence, $L$ is independent of spherical radius ($s$), so the Stefan-Boltzmann law dictates $T(s)$, and material properties are irrelevant. Temperature is constant in the core and proportional to $L^{¼}s^{-½}$ above. A point source core sets the upper limit on $T(s)$, giving $T_{\text{average}} = (6/5)T_{\text{surface}}$. Core size or convecting regions little affect our results. We also construct a parameter-free model for interior pressure ($P$) and density ($\rho$) by inserting our $T(s)$ formula into an ideal gas law ($P/\rho \propto T$) while using the equation for hydrostatic gravitational compression. We find $P \propto s^{-3}$, $\rho \propto s^{-5/2}$, and $\rho_{\text{average}} = 6 \times \rho_{\text{surface}}$. Another result, $L \propto \text{mass}^{3.3}$, agrees with accepted empirical rules for main sequence stars, and validates our model. The total solar mass already "burned" suggests that fusion occurs near $s_{\text{surf}}/400$ where $P \sim 0.5 \times 10^{12}$ Pa, in agreement with H-bomb pressure estimates. Implications are discussed.

*Keywords:* steady-state, heat transport, Stefan-Boltzmann law, stellar temperatures, stellar pressures, luminosity, effective radiative conductivity, hydrostatic compression, local thermal equilibrium, phase transitions

*Corresponding author: hofmeist@wustl.edu

## 1 INTRODUCTION AND BACKGROUND

Most stars, including our Sun, lie on the main sequence, a diverse group whose members possess masses ranging from ∼0.1 to 200 times solar. Yet, their radii, temperatures, colors, and luminosities are all related to their mass by empirical power laws [1]. This simple behavior, along with the compositional dominance of hydrogen, suggests that interiors of stars during their long, stable, main sequence stage are governed by rather few rules. In contrast, modern models of stellar interiors involve multiple assumptions and many free parameters [2–8], yet the results closely resemble Emden's [9] classical model (Figure 1a), which assumes that stars do not emit light or heat.

Furthermore, modern models give a progressive increase in luminosity ($L$) over time for the Sun [10], which is incompatible with geologic evidence (Figure 1b). The rock record indicates that Earth's surface has been dominated by liquid water for the last 4 billion years [11, 12]. Moreover, paleo-temperatures over the last 100 Ma have declined, based on robust and confirmed data [13], which strongly suggests that the Sun has cooled over this lengthy recent interval. The discrepancy between geologic evidence and the standard solar model (SSM) is important, because the model is constrained

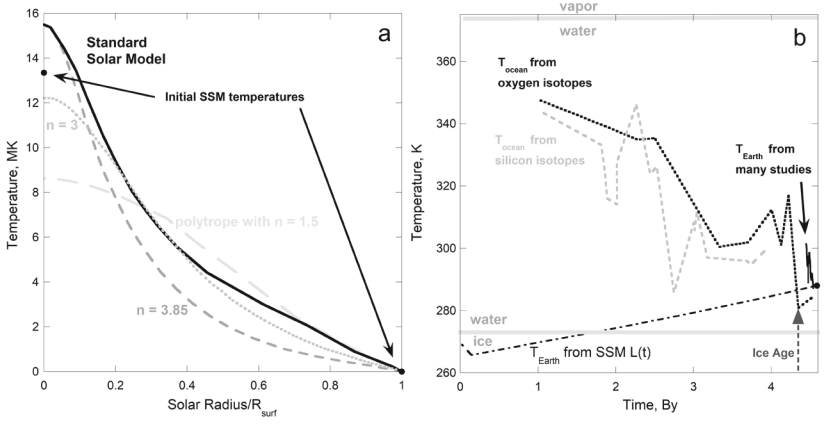


FIGURE 1
Previous models of the Sun: (a) Temperature profile from the Standard Solar Model (SSM) compared to $T(s)$ from several polytropes (the equilibrium Lane-Emden approach for non-luminous stars). An index of $n = 3 = 1/(\gamma - 1)$ gives the best overall match. The $n = 3$ polytrope (dotted curve) used the surface value of the average molecular weight, $\mu = 0.62 \equiv \rho/(\mathrm{Nm_H})$, as in the SSM (solid curve: dots show initial conditions): from [7, 10, 14]. For $n = 3.85$ (short dash), the central temperature was scaled to match the SSM. For $n = 1.5$ (long dash), the match is to the SSM surface temperature gradient; (b) Earth's declining surface temperature vs time, as indicated by geologic evidence such as isotopic data, differs greatly from the trend of increasing $T$ calculated from SSM luminosity (dot-dashed) vs time [10]. Short gray dashes from [12]; Fine dots from [11]; Thin solid curve shows robust, post-Cretaceous data [13]. Grey solid lines show water phase transitions at 1 atm.

by current observations only of the Sun's photosphere, which composes a tiny fraction of its radius [14]. Emissions result from processes much deeper inside. Moreover, experiments do not reach the inferred interior conditions, other than in transient explosions of atomic bombs, which are also modelled [15], and so cannot validate SSM calculations.

A possible source of the discrepancy between SSM calculations and geologic data is suggested by comparing assumptions underlying these modern models [2–8] with Emden's historic approach [9]. Both reasonably assume hydrostatic conditions under spherical symmetry and Newtonian physics [16]. Relevant equations are:

$$-\frac{\partial P(s)}{\partial s} = \rho(s)g(s) \tag{1}$$

where $s$ is the radius in spherical geometry, $P$ is pressure, $\rho$ is density and $g$ is gravitational acceleration:

$$g(s) = \frac{GM_{in}(s)}{s^2} \tag{2}$$

where $G$ is Newton's gravitational constant and the mass interior to any radius is defined by:

$$M_{in}(s) = \int_0^s 4\pi s^2 \rho(s) ds \tag{3}$$

All models utilize an equation-of-state (EoS), mostly that of the ideal gas, due to limited relevant experimental data.

Differences exist in assumptions for the generation of heat-energy ($Q$), heat transport, and luminosity. In summary:

- Emden's [9] polytrope model is a static, equilibrium, classical thermodynamic construct that generalizes the EoS for a perfect gas under adiabatic conditions, to depict global equilibrium (Table 1). His elegant analytical method uses two free parameters to incorporate gravitation (Equations 1 to 3) into classical thermodynamics [17], which otherwise are independent models [18]. Lack of heat flow and luminosity are compatible with presuming unrealistic values of $T = 0$ and $\rho = 0$ at the stellar surface. High internal $T$ in Emden's model results from assuming that gravitational potential was converted to heat during star formation, which is retained. This conversion is central to Kelvin's now overturned hypothesis for the origin of starlight, and neglects the fast spin of young stars [19].
- Modern models purportedly describe heat transport (Table 1), yet results closely resemble thermal profiles from classical models for non-luminous stars (Figure 1a). Because substantially different thermal gradients ($\partial T/\partial s$) are expected during heat transport than under equilibrium conditions (Sections 1.1 and 1.2), assuming local thermal equilibrium (LTE) underlies similarity of profiles. Specifically, modern models obtain $T$ from an EoS and then use this result to calculate heat transport properties [2–8],

TABLE 1
Summary of spherically symmetric models for stellar interiors

| **Description** | **Classical Model*** **(Emden-Lane Polytrope)** | **Modern Models†** **(SSM)** | **Steady-state Model‡** **(This work)** |
|---|---|---|---|
| Equation of state (EoS) | Ideal gas law plus $P = \beta\rho^{\gamma}$: $\beta, \gamma =$ constants | Ideal gas law and others | Ideal gas law |
| Governing principle | Global thermal equilibrium | Local thermal equilibrium which depends on time& | Fourier's flux ($\Im$) equation |
| Initial energy source | Interior heat ($Q$) comes from gravitational potential energy during formation | Interior heat initially from gravitational potential energy during formation | Initial conditions are immaterial in steady-state |
| Subsequent heat source | Not applicable | Nuclear reactions at depth, over a wide radius range | Heat is generated in a shell§ |
| Heat transport | Not applicable | Radiation and/or convection¶ | $\Im = \sigma_{SB} T(s)^4 = \frac{L_{surf}}{4\pi s^2}$ |
| Thermal Conductivity | Not applicable | $\kappa = \frac{4T^3}{3\rho} \times$ constants | Not assumed: $\kappa(T)$ is a result@ |
| Boundary conditions at center ($s = 0$) | $M = 0$ | $M = 0$; $L = 0$ | $L(s) = L_{surf}$ above the core; $T$ is constant in the core § |
| Boundary conditions at surface ($s = s_{\text{surf}}$) | $T_{\text{surf}} = 0$ ($L = 0$); $\rho_{\text{surf}} = 0$; $M_{\text{total}}$ | $T_{\text{surfl}}$; $L_{\text{surf}}$¥; $\rho_{\text{surf}} = 0$; $M_{\text{total}}$ | $T_{\text{surfl}}$; $L_{\text{surf}}$; $\rho_{\text{surf}}$; $M_{\text{total}}$ |
| Remarks | Two free parameters ($\beta, \gamma$); Non-luminous stars only | Many free parameters: Not validated | Zero free parameters; Replicates empirical laws; Consistent with geologic data |

*Eddington [17] provides details. Polytropes are described by index $n = 1/(\gamma - 1)$.

†This table presents the spherical, non-relativistic modern model summarized in monographs and textbooks [2–8]. The focus is the SSM: see text.

‡Time-independent heat transfer model for stable stars developed in the present paper.

&See text for discussion of this inconsistency

§Cases of a point mass source, and a variable size for the heat generating shell are explored. The results are used to suggest a mechanism for heat generation.

¶Convection is modelled by simply assuming that an adiabatic gradient exists: problems are noted by [2], see text.

@An effective $\kappa$, representing diffusion of radiation and participation of the medium (see text) adheres to Fourier's laws. Microscopic behavior is immaterial in a macroscopic model.

¥Tables of SSM results vs time [10, 14] show that the central $T$ increases while increases in the Sun's surface radius and luminosity compensate, providing $T_{\text{surf}}$ that is constant, $5000 \pm 100$ K.

rather than calculating $T$ from the equations for heat transfer. Reliance on LTE is evident in recent statements that the deviation from global thermal equilibrium is small in stellar interiors (p. 28 in [7]), and that complete equilibrium is viewed as a good approximation for the main sequence (p. 67 in [4]). Section 1.3 summarizes problems in modern models.

Section 1.4 describes our alternative analytical approach. This is based on heat transfer principles and invokes no free parameters (Table 1).

### 1.1 Thermal gradients during heat transfer

The essential equations for temperatures in regions where heat is flowing are those of Fourier. He defined flux ($\Im$, heat per area per time). Under spherical symmetry, his 1st law is:

$$\Im = -\kappa(T, s)\frac{\partial T}{\partial s} \tag{4}$$

Thermal conductivity ($\kappa$) depends on $s$ because the flow of heat is a diffusive process. After all, Fick's equations for diffusion of mass are based on Fourier's. Dependence of $\kappa$ on length-scale across layers is long-known. This also describes homogeneous materials, as recently demonstrated experimentally [20, 21].

Theoretically, the length-scale dependence of $\kappa$ is extracted from Fourier's 2nd equation, which describes variations in $T$ with time ($t$), by dimensional analysis, assuming small changes in temperature. The modern form of his "heat" equation for the sphere is:

$$\rho c_P \frac{\partial T}{\partial t} = \frac{1}{s^2}\frac{\partial}{\partial s}\left[s^2\kappa(T, s)\frac{\partial T}{\partial s}\right] + Q_{gen} \tag{5}$$

where $c_P$ is specific heat, and so the factor $\rho c_P$ is heat capacity per volume. The rightmost term addresses internal heat generation (gen), if present.

Importantly, Fourier's model is macroscopic, and thus describes the process of heat diffusion irrespective of the microscopic mechanism [22]. Misunderstandings arise from common use of the term "radiative transfer" to describe both diffusion of light where the medium plays an essential role [23, 24], as well as the entirely different process of boundary-to-boundary (or direct or ballistic) transport where the medium negligibly participates. The latter is exemplified by receipt of sunlight by the Earth. Ballistic processes occur at frequencies where the medium is transparent, and so are present in laboratory measurements to some degree, where equations in addition to Fourier's are needed [25]. Confusion also exists because convection is often stated to be a mechanism, which is untrue [26]. Instead, convection is a large scale process involving multiple mechanisms and boundary layers [27]. Lastly, "conduction" is diffusion of heat. This term is partially due to $\kappa$ from laboratory experiments at small scales and low $T$ being different than $\kappa$ from calculations of behavior at high $T$ over large scales, which has been

denoted $\kappa_{\text{eff}}$. But mostly, distinguishing conduction from radiative diffusion is a relic of considering heat (the "caloric") and visible light as different phenomena by Fourier, and many subsequent workers.

Regardless of details, Fourier's model show that $\kappa$ is the key descriptor of heat transport across some distance. Flux and heat generation are important components of his model, but commonly enter as boundary conditions. Section 2 covers circumstances in stars.

### 1.2 Incompatibility of LTE with heat transfer, including radiative processes

Use of LTE in stellar models originated with Eddington circa 1926, who incorrectly stated that during equilibrium, heat flows via diffusion (pp. 97ff in the later edition [17]). Instead:

- The 0th law of thermodynamics states that systems in equilibrium have the same temperature, so thermal gradients are null and net heat flow is impossible.
- The Stefan-Boltzmann law:

$$\Im = \sigma_{SB} T^4 = \frac{L}{4\pi s^2} \tag{6}$$

  corroborates that objects with different temperatures cannot be in thermal equilibrium, regardless of whether communication is across space (ballistic radiation) or via physical contact. Misunderstanding LTE in stars in part arises from misuse of the term "radiative equilibrium" to describe Earth's surface temperature being maintained by the solar flux. Instead, the situation is "radiative steady-state" because Earth's receipt of solar radiation is balanced dynamically by its radiative losses to space.
- According to Equations (4) and (6), net heat flows requires that temperature differences exist, which may be incremental, and thus describes disequilibrium. Consequently:
- Even during steady-state conditions, where heat flows steadily, but the system does not thermally evolve, using the LTE approximation is inappropriate [28].

Figure 2a illustrates these four points. At the junctions between any two adjacent intervals, each of which is represented by an equilibrium state, the heat flux is infinite, so each junction is a site of profound disequilibrium. Notably, disequilibrium leading to convection, where mass and heat both move, is manifest not in the adiabatic gradient of the circulating interior, but in the boundary layers (Figure 2c; [27]).

A related misunderstanding of radiative processes is found on p. 104 of [17]: "Equation 71.1 shows that the net flow of radiation is, as we should expect, proportional to its internal pressure gradient." Eddington's equation,

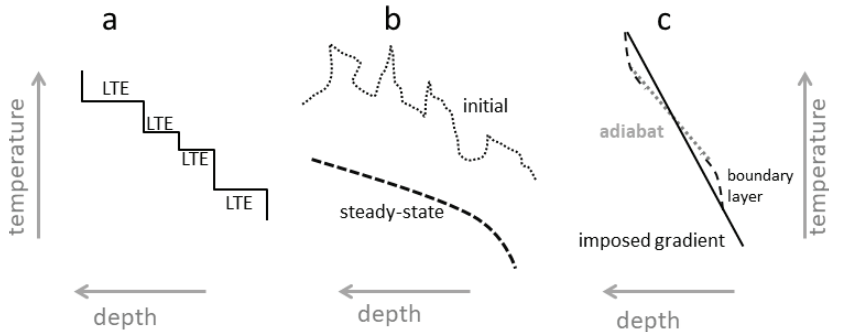


FIGURE 2
Schematics: (a) The LTE approximation specifies thermal equilibrium in limited zones, but not over the aggregate region, nor does LTE prescribe how adjacent zones are linked, so the regional thermal gradient is undefined; (b) Evolution of temperature in a system starts from some initial condition (dotted curve), but this is unrelated to the gradient achieved in steady-state (dashed curve) and likewise the process of reaching steady-state is unrelated to the achieved thermal gradient; (c) Convective instability occurs when imposed thermal gradients are steeper than an adiabat. Most of the temperature change occurs at the boundary layers, as documented in laboratory settings [27], where the circulating centers are isothermal.

and thus his model, fails to recognize that any amount of light can coexist in some volume. That flowing heat itself is not affected by pressure is experimentally confirmed: only the medium is compressed [21].

### 1.3 Synopsis of modern model shortcomings

Although Emden [9] clearly stated that his polytrope model applies only to non-luminous bodies, it has been widely applied to shining stars [8]. Misunderstandings of Eddington (mentioned above) are apparently the source. Roxburgh's [2] statement "Such models are, at best, only a first approximation, and at worst, totally misleading" has been forgotten. However, evaluating the details in multi-parameter modern numerical models (Table 1) is unnecessary, given multiple overarching incompatibilities:

- Deviations of SSM from polytropes are small, yet the historic model permits no heat flow.
- Evolution is a unidirectional, disequilibrium phenomenon that is wholly incompatible with LTE. Consequently, SSM results are incompatible with geologic evidence (Figure 1b).
- An evolutionary model need not converge to a steady-state condition: nor does convergence of the calculations prove that LTE is a reasonable approximation. Once steady-state is reached, time is irrelevant (Figure 2b).
- Convection results from a large-scale instability and cannot occur under LTE. All convective systems have boundary layers ([27]; Figure 2c), yet the smooth SSM $T$ profiles provide no evidence for boundary layers (Figure 1a). Smooth profiles exist because model construction proceeds

by integrating from the center outward, and independently integrating from the surface inward, and iterating until convergence is met at some convenient interior point deep inside the star [3] (p. 87).

### 1.4 Purpose, organization, and encapsulation

We develop a new class of models for stellar interiors that incorporates their internal flow of heat and its manifestation as starlight. In Fourier's macroscopic model, it is immaterial whether heat is transferred microscopically via electrons, phonons, or photons [22]. Temperature governs stellar interiors because $\rho$ and $P$ respond instantaneously in the elastic approximation (Figure 3a; [29, 30]). Convection is a system-wide response to an imposed temperature gradient that is too large for heat to diffuse when the medium is too weak to resist material flow [27]. One goal of the present paper is to establish $\partial T/\partial s$, which permits probing if convecting regions could exist.

Because main sequence stars are considered to be stable for long periods of time, steady-state heat flow is an appropriate depiction. During steady-state, $\partial T/\partial t = 0$, even though energy is continuously generated. Hence, only Equation (4) is needed. This simple formula, spherical symmetry, plus Stefan-Boltzmann's law (6) make the heat transfer problem of interior stellar temperatures tractable.

Our macroscopic approach shares a major advantage of thermodynamics, as it requires no special assumptions concerning the nature of matter, yet yields straightforward, testable predictions that can disclose theoretical connections between measurable quantities [22]. Validation is part of such endeavors. Key features of our new class of models are:

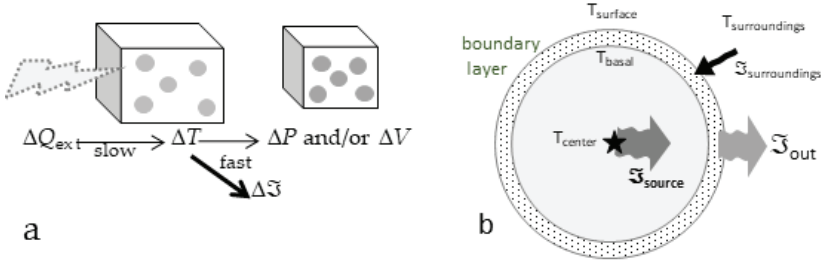


FIGURE 3
Schematics illustrating basic physical principles utilized here: (a) Receipt of a small amount of heat by matter. Within a short but finite distance, the pulse encounters an atom or ion. When energy of the applied light matches some transition energy, a higher energy state is attained. Subsequent interchanges impart an overall higher energy to the collection, causing temperature to rise. Both steps take time and reaching an equilibrium $T$ requires time as well. However, the accompanying $P$, $V$ changes are instantaneous in a conservative, elastic system; (b) Heat flow across a cross-section of a sphere. Matter (grey circle) emits heat in accord with its temperature (grey squiggle arrow), but emissions actually emerge from a boundary layer below the surface (stippled shell): see text or [20]. Steady state is achieved when losses (squiggle arrow) balance inputs (black arrow) plus internal heat generation (star and large squiggle arrow). Modified after [29], which has a creative commons license.

- Our approach is unlike existing models, in which temperatures are controlled by the assumed EoS and the chosen parameters.
- Our analytical model (Section 2) has no free input parameters and only uses proven physical laws and standard physical constants (Table 2).

TABLE 2
Physical constants and solar properties* used as inputs in our parameter-free, hydrostatic, steady-state model

| **Constants** | **Symbol** | **Value** | **Solar Properties**† | **Symbol** | **Value** |
|---|---|---|---|---|---|
| Gravitational constant | $G$ | $6.674 \times 10^{-11}$ m$^3$ kg$^{-1}$s$^{-2}$ | Mass | $M_S$ | $1.989 \times 10^{30}$ kg |
| Stefan-Boltzmann constant | $\sigma_{SB}$ | $5.67 \times 10^{-8}$ W m$^{-2}$K$^{-4}$ | Average radius | $s_{\text{surf}}$ | 695700 km |
| Gas constant‡ | $R_{gc}$ | 8.314 J mol$^{-1}$ K$^{-1}$ | Luminosity§ | $L_S$ | $3.83 \times 10^{26}$ W |

*Sources are various, e.g., [1].
†Solar ellipticity, $e = 0.00005$, but is not used.
‡This constant is only used to describe the surface pressure from the atmosphere in our model.
§This luminosity provides surface temperature of 5775 K via Equation (6).

Three steps are taken in Section 2: First, temperature vs depth is ascertained from heat transfer formulae. Second, the hydrostatic equation is used to quantify compression inside the star. Third, the ideal gas EoS is used to depict the *PV* response of supercritical fluid to self-gravitation. We explore various surface densities, which addresses the fact that images of the Sun show a surface distinct from its rarified atmosphere. Core size is explored, but has no effect on most of the stellar interior. Mass-luminosity empirical laws provide validation.

Surface solar values are accurate and complete (Table 2), permitting detailed analysis of the Sun's interior in Section 3. Our results are supported by available constraints. In short, our work takes Fourier's model and Stefan-Boltzmann's law to the logical conclusion that temperatures inside stars are inversely proportional to the square-root of radial distance. The increase in $T$ towards the center that is both specified and required by this equation is weak compared to that predicted by previous LTE models, which has many ramifications (Sections 4 and 5).

## 2 THEORY

### 2.1 Conservation Laws

Nuclear reactions in normal stars release prodigious amounts of energy, yet proceed at a very low rate. Thus, the small mass loss associated with energy

production can be neglected in a steady-state model. Because heat generated balances heat output in steady-state, our model conserves heat-energy separately than mass.

## 2.2 Occupation of space by energy

When heat is incrementally added to a system, it strives to regain equilibrium by increasing its temperature (Figure 3a). Thereafter, $P$ and $\rho$ respond, in accord with the physical conditions and material properties. Hence, stellar interior temperatures must be ascertained first.

### *2.2.1 Temperatures in stable stars with a point source*

Under spherical symmetry and steady-state conditions, the amount of energy that enters and leaves each interior shell must be equal, as implied in Figure 3b. Since $\Im$ is energy per area per time, (6) becomes:

$$T(s) = \frac{1}{s^{1/2}}\left(\frac{L_{surf}}{4\pi\sigma_{SB}}\right)^{1/4} \quad \text{so} \quad T(s) = T_{surf}\left(\frac{s_{surf}}{s}\right)^{1/2} \tag{7}$$

Equations (6) and (7) describe a blackbody, an ideal case with emissivity and absorptivity = 1, so reflectivity and transmissivity = 0, after Kirchhoff. These conditions are assumed to connect star color to surface temperature [31]. More importantly, blackbody radiation is the entity diffusing inside stars. The required condition is that light is absorbed and reemitted within a distance shorter than that over which $T$ changes significantly [23, 24, 32]. This condition is commonly met inside large bodies, but not necessarily in the laboratory [25].

Temperature approaches infinity at the center (Equation 7). This singularity has little effect because a point occupies null volume. Accordingly, the volumetrically averaged $T$ is bounded even in that case:

$$T_{average} = \frac{\int_0^{s_{surf}} 4\pi r^2 T(r)dr}{\int_0^{s_{surf}} 4\pi r^2 dr} = \frac{3}{{s_{surf}}^3}\left(\frac{L}{4\pi\sigma_{SB}}\right)^{1/4}\int_0^{s_{surf}} r^{3/2}dr = \frac{6}{5}T_{surf} \tag{8}$$

### *2.2.2 Steady-state heat transfer in stars with finite size core*

Stellar energy could be generated within some shell of finite radius. We approximate this shell as being thin. Consequently, the shell defines $s_{\text{core}}$, which overlies an inactive (spent) core. Hence, (7) holds above $s_{\text{core}}$, and $T$ of this shell defines the constant $T$ of the underlying core during steady-state heat flow:

$$\text{For} \quad s \le s_{core},\ T = T_{core};\ \text{and for } s > s_{core},\ T_{average} = \frac{6}{5}T_{surf}\left[1 - \frac{1}{6}\frac{{s_{core}}^{5/2}}{{s_{surf}}^{5/2}}\right] \tag{9}$$

where the LHS was obtained from Equations (7) and (8). Employing (9) requires independent knowledge of core size. Because core sizes are currently model values, Section 3 explores a wide range of core sizes.

*2.2.3 Consequences for thermal conductivity*

Considering steady-state and spherical symmetry yielded $T(s)$ without assuming specific behavior nor specific values for $\kappa$. Consequently, combining (4) and (6) stipulates $\kappa$:

$$\kappa(T) = T\left(L\sigma_{SB}/\pi\right)^{1/2}, \text{ where } T = T(s) \text{ from Equation (7)} \tag{10}$$

Equation (10) holds for all $s$, but is irrelevant inside the constant $T$ core.

Equation (10) does not actually depict a material or spectroscopic property because the temperature therein is controlled by radial distance in the sphere, not by a specific mechanism, which is a consequence of the definitions of flux and luminosity. It is the geometry of the sphere and the special condition of steady-state which permits extraction of $T$ independent of such details, and defines the above effective $\kappa$. Sections 4.1 and 4.5 provide discussion.

## 2.3 Occupation of space by mass

The reaction of matter to heat is generally slow, while its elastic response is considered instantaneous (Figure 3b; [29, 30]). Likewise, action at a distance (gravitation) is essentially instantaneous. Consequently, $P$ and $\rho$ are secondary responses to $T$ whenever heat transfer occurs.

*2.3.1 Containment of matter in a hydrostatic star*

Hydrostatic conditions are governed by Equations (1) to (3), which combine to provide:

$$-\frac{\partial P(s)}{\partial s} = \rho(s)g(s) = \rho(s)\frac{GM_{in}(s)}{s^2} = \rho(s)\frac{G}{s^2}\int_0^s 4\pi r^2\rho(r)dr \tag{11}$$

Equation (11) defines how the spherical shells of a self-gravitating star occupy space. It specifies the trade-offs between $V$ (or $\rho$) and $P$ at each and every radius that has some specific temperature, where $T$ is governed by heat transfer (Section 2.2).

Also, and by definition:

$$\rho_{avg} = \frac{M}{4/3\,\pi s_{surf}^3} \tag{12}$$

*2.3.2 Response of matter to compression*

The EoS of any material is defined by its physical properties of compressibility ($\beta =$ the inverse of the bulk modulus) and thermal expansivity ($\alpha$), which describe responses of the material to each of $P$ and $T$:

$$\beta_T \equiv -\frac{1}{V}\frac{\partial V}{\partial P}\bigg|_T = \frac{1}{\rho}\frac{\partial \rho}{\partial P}\bigg|_T = \frac{1}{B_T} \quad \text{and} \quad \alpha_P \equiv \frac{1}{V}\frac{\partial V}{\partial T}\bigg|_P \tag{13}$$

Because (13) depicts change in $V$, not shape, hydrostatic conditions are described [29].

To complete our description of stellar interiors, the form, $f(P, V, T) = 0$, is needed. The ideal gas law describes experiments on gases, particularly if composed of tiny atoms (He or H) or molecules ($H_2$):

$$PV = NR_{gc}T \qquad \text{or} \qquad \frac{P}{\rho} = \frac{R_{gc}}{m}T \tag{14}$$

where $m$ is the molar mass and $R_{gc}$ is the gas constant. The ideal gas law, without the proportionality constants, can be extracted from the Virial theorem [19], so the form of (14) is quite general.

Other EoS could be incorporated in our approach. If the form reduces to $P/\rho \propto T$, the results will not be altered, since proportionality constants cancel for this form: see below.

We qualitatively explore the van der Waals formulation because this takes the finite size of atoms into account. In its simplest, original form:

$$P(V - V_0) = NR_{gc}T \tag{15}$$

where $V_0$ is the excluded volume [33].

Should excluded volume exist, contraction halts at some high pressure. Such essentially incompressible behavior promotes a phase transformation to a state which is not only denser, but can contract (e.g., from the rock-salt to CsCl structure, which has a higher coordination number, where the longer bonds are weaker). Such behavior is commonly exhibited in solids [34]. Hence, Equation (15) proxies for solids that might exist deep in a star. However, because conditions in stellar interiors are unconstrained by experiments or measurements, we only discuss the consequences, but do not use (15) in computations.

## 2.4 Interiors of main sequence stars

Our model assumes that any region of interest is sufficiently small that $P$ and $\rho$ are uniform. But, simultaneously, a sufficient number of molecules must exist in volume $V$ to provide a statistical average. Because stars are immense, statistical requirements are met in each of the nested shells.

*2.4.1 Behavior of an ideal gas star*

Inserting $T(s)$ from Equation (7) into the EoS relates pressure to density, radius, surface luminosity, and some constants, which combine into a single "const":

$$P(s) = \frac{\rho(s)}{s^{1/2}} \frac{R_{gc}}{m} \left( \frac{L}{4\pi\sigma_{SB}} \right)^{1/4} \equiv const. \frac{\rho(s)}{s^{1/2}}. \tag{16}$$

To eliminate pressure, we take the derivative of Equation (16) and insert this result into the RHS of the hydrostatic formula, Equation (11). A simple integral equation results:

$$const. \left[ s^{-1/2} \frac{\partial \rho}{\partial s} - \frac{\rho}{2} s^{-3/2} \right] = 4\pi G \frac{\rho}{s^2} \int_0^s r^2 \rho(r) dr \tag{17}$$

Rearranging gives:

$$\frac{4\pi G}{const.} \int_0^s r^2 \rho(r) dr = \left[ \frac{s^{3/2}}{\rho} \frac{\partial \rho}{\partial s} - \frac{1}{2} s^{1/2} \right] \tag{18}$$

Taking the derivative of (18) gives:

$$\frac{4\pi G}{const.} s^2 \rho = \left[ \frac{3}{2} \frac{s^{1/2}}{\rho} \frac{\partial \rho}{\partial s} + \frac{s^{3/2}}{\rho} \frac{\partial^2 \rho}{\partial s^2} - \frac{s^{3/2}}{\rho^2} \left( \frac{\partial \rho}{\partial s} \right)^2 - \frac{1}{4} s^{-1/2} \right] \tag{19}$$

Dividing by $s^2$ and then rearranging terms produces:

$$\frac{4\pi G}{const.} = \left[ \frac{3}{2} \frac{1}{\rho^2 s^{3/2}} \frac{\partial \rho}{\partial s} + \frac{1}{\rho^2 s^{1/2}} \frac{\partial^2 \rho}{\partial s^2} - \frac{1}{\rho^3 s^{1/2}} \left( \frac{\partial \rho}{\partial s} \right)^2 - \frac{1}{4} \frac{1}{\rho s^{5/2}} \right] \tag{20}$$

Because the LHS of (20) is a constant, each term on the RHS must likewise be constant. All terms are dimensionally identical. Because density must inversely respond to radius, the solution to (20) is:

$$\frac{\rho(s)}{\rho_{surf}} = \left( \frac{s_{surf}}{s} \right)^{5/2} \tag{21}$$

which incorporates the boundary condition of $\rho = \rho_{\text{surf}}$ at $s = s_{\text{surf}}$. Algebraic manipulation relates surface density to the constants defined in Equation (16):

$$\rho_{surf} = \frac{1}{s_{surf}^{5/2}} \frac{3}{8\pi G} \frac{R_{gc}}{m} \left( \frac{L}{4\pi\sigma_{SB}} \right)^{1/4} \tag{22}$$

which presumes the ideal gas proportionality constant ($R_{gc}/m$) holds throughout the star, and that the surface is not controlled by some phase boundary, discussed further below.

Irrespective of any possible constraint on $\rho_{surf}$, interior mass is obtained from combining Equations (3), (12), and (21):

$$M_{in}(s) = 8\pi\rho_{surf}s_{surf}^{5/2}s^{1/2} = 6M\frac{\rho_{surf}}{\rho_{avg}}\sqrt{\frac{s}{s_{surf}}} \quad \text{and thus} \quad \rho_{surf} = \frac{1}{6}\rho_{avg} \tag{23}$$

which represents the solar interior, not its atmosphere. Importantly, the far RHS of (23) is independent of the ideal gas proportionality constants, and only requires $P/\rho \propto T$.

Combining Equation (16) with (21) specifies pressure:

$$P(s) = P_{surf}\left(\frac{s_{surf}}{s}\right)^3 \text{ where } P_{surf} \text{ is derived from the weight of the atmosphere} \tag{24}$$

Equation (24) states that the product PV is constant at any given spherical radius. It is a consequence of the occupation of space by matter being independent of its occupation by energy, which defines $T$ in the shell.

The average pressure is computed from the average radial position ($¾s_{surf}$) and Equation (24), yielding a simple, finite value for a point-mass core:

$$P_{avg} = P_{surf}\left(\frac{s_{surf}}{s_{avg}}\right)^3 = \frac{64}{27}P_{surf} \tag{25}$$

Steps similar to the above provide the internal gravitational acceleration:

$$g(s) = g_{surf}\left(\frac{s_{surf}}{s}\right)^{3/2} : \text{where } g_{surf} = \frac{GM}{s_{surf}^2} \tag{26}$$

Some central values in the point-source models involve singularities. All singularities exist only at the zero-volume point, and so do not affect the averages.

The reduced moment of inertia for normal stars with tiny cores in the ideal gas approximation is:

$$I_{reduced} = \frac{I}{Ms^2} = \frac{1}{Ms^2}\frac{2}{3}\int_0^s r^2 dm = \frac{8\pi}{3Ms^2}\int_0^s r^4\rho(r)dr = \frac{2}{15} = 0.133 \tag{27}$$

*2.4.2 Implications of atoms having finite size on stellar cores*

If the excluded volume of Equation (15) is reached exactly at the star's center, then a prescription for density can be obtained using procedures similar to those above for the ideal gas stars. The result (not shown) closely resembles that of ideal gas. Although a van der Waals star involves an unknown central density ($V_0 = m/\rho_{center}$), this isopycnic condition resembles the isothermal condition required during steady-state. Hence, our applications below consider

ideal gas behavior above the radius of heat generation, and explore various sizes for the core defined by this shell. Each core size has a central density that can be approximated as a constant from Equation (21). Central pressures can be likewise approximated from Equation (24). Central temperatures are exactly constant (Section 2.2).

### 2.5 A simple derivation of power laws for steady-state stars

The two leftmost terms of (23) and (22) respectively reduce to two proportionalities:

$$M \propto \rho_{surf} s_{surf}^3 \quad \text{and} \quad L^{1/4} \propto \rho_{surf} s_{surf}^{5/2} \tag{28}$$

All factors omitted are physical constants. The RHS of (28) is valid for any proportionality constant in the ideal gas law (14) and further assumes only steady-state and hydrostatic conditions. If $\rho_{\text{surf}}$ is also a constant, i.e., is the same for all main sequence stars because star surfaces are controlled by a phase transition between their opaque dense interior and transparent, rarefied atmosphere, then:

$$L \propto M^{10/3} : \text{ specifically, } \frac{L_{star}}{L_{Sun}} = \left( \frac{M_{star}}{M_{Sun}} \right)^{10/3} \tag{29}$$

Under constant $\rho_{\text{surf}}$, combining Equations (28), (6) and (29), yields:

$$\frac{T_{star}}{T_{Sun}} = \left( \frac{M_{star}}{M_{Sun}} \right)^{2/3} \qquad \text{and} \qquad \frac{s_{star}}{s_{Sun}} = \left( \frac{M_{star}}{M_{Sun}} \right)^{1/3} \tag{30}$$

Hence, $L$, $s$, and $T$ at stellar surfaces directly depend on the enclosed mass.

Our simple derivation provides the well-known empirical power laws that describe main sequence stars. Previous explanations make many assumptions and use about 10 mathematical manipulations to arrive at these empirical formulae [16, 35]. Extracting the power laws in a simple manner validates our steady-state model.

## 3 RESULTS FOR THE THERMALLY STABLE SUN

### 3.1 Solar Temperatures

Under steady-state conditions, temperatures in the Sun's interior are specified by $L$ and $s_{\text{surf}}$ (Section 2.2). No free parameters are used. The surface value of 5775 K from luminosity is similarly obtained: this is known as the effective temperature [31].

The model is singular in $T$ at $s = 0$ (the point source). Yet, over most of the stellar volume, $T(s)$ is remarkably low, resembling the average value which differs little from $T_{\text{surf}}$ (Figure 4). Hot regions occur only near and within the tiny central zone. For example, a small core, constituting 0.1% of the Sun's

volume, would have temperatures only 3.15 times that at the surface. A huge core, where heat is generated in the shell at ½ of the surface radius (i.e., at the surface of a core with ⅛th of the total volume), would have a core temperature only 1.41 times $T_{surf}$ (Figure 4).

Since point sources do not exist, heat generation occurs at some finite radius. This radius ($s_{core}$) is described by a certain $P$ and $T$, because fusion changes the state of the atoms, and thus shares some features with phase transitions explored in the laboratory (Section 4.5). In steady-state, the core is isothermal. Because core temperature depends on core radius, the volumetric average of $T$ over the whole Sun also depends on $s_{core}$ (Figure 5). The average $T$ of the star remains near 6930 K for cores of nearly negligible size to large cores extending out to ¼th of $s_{surf}$ ($\sim$1.6% of the total volume). Thus, interior temperatures are not greatly elevated compared to surface temperatures for stars that are thermally stable. If the core is large, the change in $T$ with depth is quite small (Figures 4 and 5).

Temperatures are limited, even for a star with a miniscule core, because stellar radiation sheds interior heat. From Figures 4 and 5, exploring a few core sizes suffices to describe interior $T$ for a star during steady-state. Consequently, a few core sizes also suffice to explore core $\rho$ and $P$.

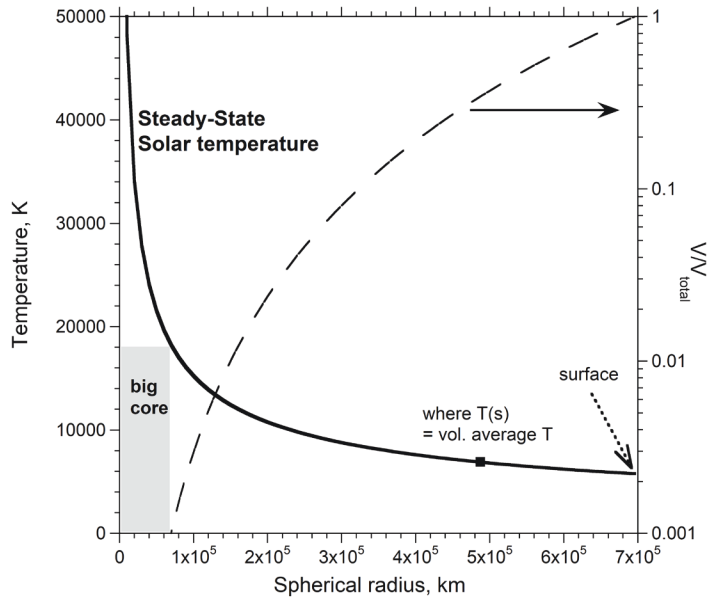


FIGURE 4
Interior temperature of the Sun from Equation (7), using accepted $T_{surf} = 5775$ K, and Equation (8), which provides the volumetric average of 6930 K for a point source. A logarithmic scale was used for the volume fraction (dashed line, right y-axis).

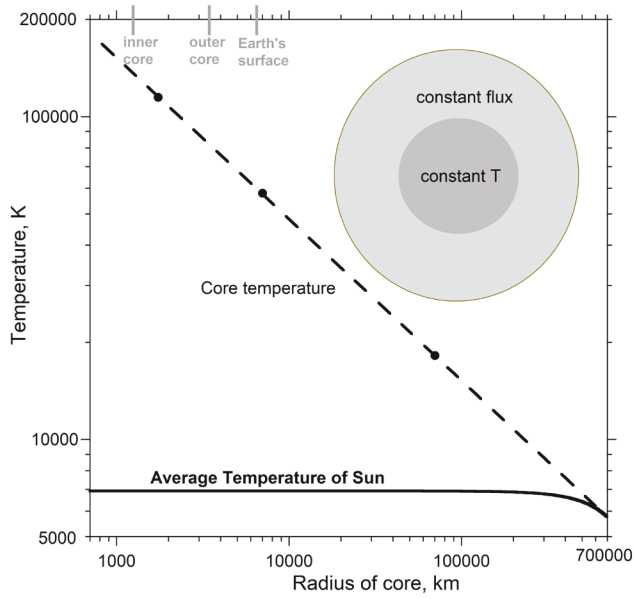


FIGURE 5
Temperatures inside a steady-state Sun with a core, shown as a function of core radius. Scales are logarithmic. The inset summarizes heat flow conditions during steady-state. Core temperatures from Equation (7). Average $T$ for the whole Sun from Equation (9). Dots show core sizes of 0.1, 0.01, and 0.0025 of the surface radius as discussed in the text. Gray bars (upper x-axis) show radii of boundaries in the Earth [36] for comparison.

### 3.2 Solar core sizes suggested by various observations

We consider core radii of 0.1, 0.01, and 0.0025 times the surface radius. These values are spaced roughly by order-of-magnitude, but moreover correspond to physically plausible situations:

A minimum core radius is indicated by production of $6.05 \times 10^{11}$ kg of He per $s^{-1}$ from fusion of H. This numerical value is computed from solar luminosity. Over 4.5 billion years, this nuclear reaction could have created a spent, He-rich region with a mass about 4% of the Sun's total. However, due to internal densification (Section 3.3.4), this sequestered mass would occupy only $\sim 2 \times 10^{-8} V_{\text{total}}$, which in round numbers corresponds to $s_{\text{surf}}/400$ ($= 1739$ km). Our estimated minimum is smaller than Earth's molten outer core (3480 km [36]), which planet is miniscule compared to the Sun.

The mass burning estimate of core size is a minimum in part because iron and other dense metals could have segregated downwards. The measured iron content of the Sun in the photosphere (0.01% [37]) sets a reasonable maximum for the core radius as $\sim 0.1 s_{\text{surf}}$, because other heavy elements detected in the outer layers are similarly abundant.

A core size of $0.01 s_{\text{surf}}$ lies between our maximum and minimum estimates. For completeness, some graphs show a core radius of $0.001 s_{\text{surf}}$ ($= 700$ km)

which is smaller than Earth's solid inner core (1221 km [36]), and has a volume only $10^{-9}$ times the whole Sun. Such a miniscule core approximates a point mass.

### 3.3 Density inside the Sun

#### *3.3.1 Observations of the solar surface*

A distinct surface is a discontinuity between different types of matter. Surfaces are commonly defined by a phase transformation. For example, Earth's oceanic surface is defined by a phase transition between water and atmospheric water vapor, because Earth is too warm for its major atmospheric components ($N_2$, $O_2$, $CO_2$) to condense. As another example, the spherical boundary between Earth's inner and outer cores is defined by the melting point of iron alloy at high $P$ and $T$ [36].

Visually, the Sun has a distinct surface, as evidenced by its granularity [38], which is interpreted as convection cells. The images point to a liquid state defining this interface for two reasons:

- Visually observing granularity requires that light from this surface is largely transmitted through the overlying atmosphere. Conversely, light is largely absorbed by the granules and below. Contrasting optical properties and $\rho$, which are linked, are required to detect an interface. Visually observing a surface requires reflection from the surface (Snell's law), but gas lacks this property. It is immaterial that emitted light from the Sun is being recorded because light originating from deeper is back-reflected at the surface of a liquid or solid [32], as demonstrated experimentally (reviewed in chapter 2 of [20]). Conservation of energy is central to Bates' [32] derivation.

Conditions in the Sun are consistent with a rarified gaseous atmosphere overlying a liquid ocean. This transition is regulated by a phase boundary.

Also germane is the single value for the radius in Table 2, which relates the luminosity to an effective temperature [31]. This determination applies (6) to the light flux received from the photosphere. In this ~500 km thick outer layer, temperatures are considered to increase with depth [39], but given the size of the Sun, the photosphere constitutes an infinitesimal outer shell. Some additional discussion is needed regarding this interface, as follows:

#### *3.3.2 Model values for surface density and pressure*

At low $P$ and high $T$, hydrogen gas should be dissociated, as detailed below. A gas composed of atomic hydrogen should follow the ideal gas EoS. Introducing values in Table 2 into Equation (22) yields $\rho_{\text{surf}} = 0.176$ kg m$^{-3}$ for the base of the solar atmosphere resting on the glowing, granulated surface defined by $s_{\text{surf}}$. At its surface temperature of 5775 K, the corresponding $P_{\text{surf}}$ is 85 bar = 0.0085 GPa, from the ideal gas law (15).

In contrast, density of the distinguishable surface of the self-gravitating body is set not by the EoS, but by the RHS of Equation (23) giving 233 kg $m^{-3}$. High $\rho_{surf}$ is consistent with measured density of cryogenically liquefied $H_2$ ranging from 70 to 86 kg $m^{-3}$ over its stability field at 1 bar [40]. Data seems unavailable on any form of hydrogen near 5775 K, see below.

Deduction of $P$ at the base of the overlying atmosphere from the EoS as $P_{surf} = 85$ bar $= 0.0085$ GPa assumes abrupt termination of the atmosphere at the granules. Alternative estimates are given below.

*3.3.3 Possible surface conditions from experiments and phase boundaries*

The Sun's surface is currently considered to be supercritical fluid H, based on confirmed dissociation experiments of $H_2$ at 1 bar [41]. Reaction kinetics pertain: at 1 bar and 3000 K, 68% dissociation was measured. From modelling his data, Langmuir [41] suggested that hydrogen would be >99% dissociated by 5000 K. His tables suggest an uncertainty of ±500 K.

Due to kinetics of reaction and the known gradation of the photosphere, both H and $H_2$ should be present in this interfacial layer. Detecting $H_2$ remotely is problematic because it lacks infrared inactivity. From indirect evidence, a recent study of sunspots suggested the presence of $H_2$ [42]. Their finding supports the Solar surface being a phase boundary where dissociation is ongoing. Although hydrogen is well studied, high-$T$ dissociation studies are made at low $P$, focusing on kinetics [43], whereas other types of experiments and calculations have focused on either $P < 2000$ bars $= 0.2$ GPa for practical matters [40] or $P > 10$ GPa [44] for science interests.

Only the review paper of McMahon et al. [44] provides a phase boundary between H and $H_2$ super-critical fluids for $P$ between ∼1 atm and 10 GPa, stating that their curve is an estimate. No details are given. The fluid-fluid transition at 5775 K was estimated as 230 bar. At 4900 K, the estimated transition is near 85 bar. Their positive slope for $\partial T/\partial P$ of the fluid-fluid transition is in accord with fluid $H_2$ being the denser phase, since covalency shrinks the H–H bond [45], and an endothermic transition.

Under steady-state, solar temperature changes much more slowly with radius than pressure changes with radius, with respect to their surface values, cf. power laws of (7) and (24). Therefore, crossing the surface downwards means that the material is being compressed more than being warmed. We conclude that fluid H in the atmosphere is transformed to fluid $H_2$ in the photosphere.

However, as discussed above, the visually observed granulated surface requires a strong density contrast, far larger than the difference inferred from the ideal gas EoS for supercritical fluids of H and $H_2$. Equation (23) for the solar surface provides this strong density contrast with the ideal gas description of the atmosphere. Notably, liquid-liquid transformations exist for many substances, with rather complicated phase boundaries [46].

The large surface gravity of the Sun, 275 m $s^{-2}$, should permit retention of a substantial atmospheric mass, providing much higher surface pressure than exists on the tiny Earth (1 bar). Interestingly, $P_{surf} = 230$ bar is provided by an atmospheric mass of $10^{-6}$ $M_{solar}$; a similar fraction describes the relation between Earth and its atmosphere.

Modelling the solar atmosphere is beyond the scope of this report. Because the estimate of 230 bars differs substantially from Langmuir's experiments at 1 bar, our calculations for the Sun focus on an intermediate surface value of 85 bars (Section 3.3.2), as observed for Venus. Variations from our model density of 233 kg $m^{-3}$ are likewise explored to gauge sensitivity of interior profiles to surface conditions.

### *3.3.4 Interior density and pressure in the Sun*

Using an EoS similar to the ideal gas yields a strong power law increase of $\rho$ as $s$ decreases and a stronger power law for $P$ on $s$ (Figure 6a). Known, finite atomic size is embodied in the presence of a core.

Only Earth provides a substantive comparison, since its interior is constrained by seismologic studies together with laboratory measurements at appropriately elevated $P$ and $T$ [36]. The Earth and Sun have much different compositions and surface temperatures, but both are self-gravitating and hot inside. Temperatures in Earth's core are ascertained from melting equilibria and are affected by impurity content, so uncertainties exist even for our well-studied planet [36]. The largest Solar core considered, consistent with the Sun's iron metal content, is about 1000 times denser than cryogenically frozen hydrogen or about 7 times denser than Earth's iron core. Thus, conditions in Earth's core do not greatly differ from our model for a

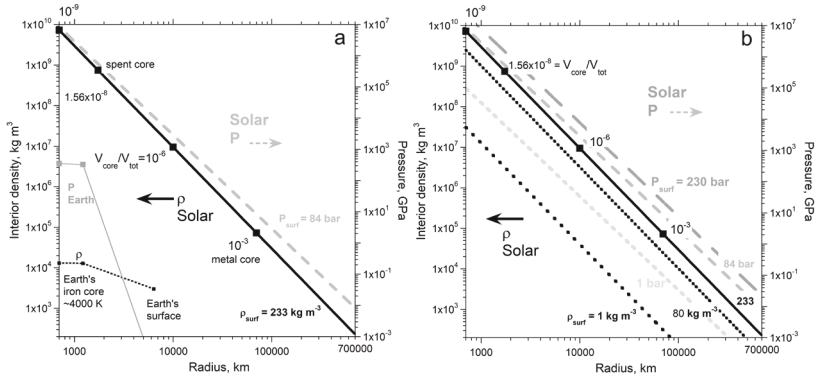


FIGURE 6
Density (left axis) and pressure (right axis) inside the Sun, calculated from Equations (21) and (24). Core sizes under consideration are shown on the density trend for a surface value of 233 kg $m^{-3}$ constrained by our model and average density: (a) Comparison with conditions in the deep Earth, where values are from seismic analysis [36]. Solar pressures start at 85 bar, constrained by the ideal gas coefficients; (b) Comparison with other surface values (see text).

compositionally stratified Sun with an iron core. Rough correspondence supports our steady-state, hydrostatic model, but does not require that the Sun's core is an iron alloy.

Figure 6b shows the effect of varying surface density and pressure from model constraints and estimates of $P_{surf}$ on the Solar interior. Because surface pressure is controlled by the mass of the atmosphere, and the interface is gradational, $P_{surf}$ is decoupled from $\rho_{surf}$, which represents the Sun immediately below the interface evident in granulation.

The surface density cannot significantly exceed 233 kg m$^{-3}$ from Equation (23), because the Sun's interior is compressed and its average density is only 1400 kg m$^{-3}$. An interior based on the lower density of cryogenic fluid ($\rho_{surf}$ estimated as 80 kg m$^{-3}$) is less compressed than our parameter-free model, but not inordinately so. From Figure 6b, modest variations in $\rho_{surf}$ are immaterial. However, a rarified start (1 kg m$^{-3}$) provides a substantially less dense interior. This situation is implausible, if not impossible, because it predicts an interior density only exceeding that of Earth's core when $s < \sim$20,000 km. Low surface density can be ruled out.

Similarly, a pressure of only 1 bar at the Sun's surface would provide a low central pressure similar to that of Earth's core, and so is also implausible to impossible. Although higher surface pressures cannot be ruled out, 85 bar seems most consistent with scant available data, as follows:

### 3.4 Pressure-temperature conditions in the Sun

Figure 7 shows calculated *P-T* conditions in the solar interior, using $P_{surf} = 85$ bar. Because the Sun is more compressed than heated, the interior may contain $H_2$, which is denser than H under the same conditions, due to covalent bonding. Further experimental constraints are lacking. Because temperatures are high, dissociation is expected, so the fusion model described in Section 4 considers H as the dominant species.

Temperature changes slowly in the solar interior. A least squares fit to the trend in Figure 6 provides the solar temperature profile:

$$T = 12782P^{0.16667} = 12782P^{1/6}, \tag{31}$$

for $T$ in K and $P$ in GPa. This holds down to the isothermal core. The core is further approximated as being isobaric and isopycnic, in lieu of independent constraints.

#### *3.4.1 Comparison of P, T results for the Sun to experiments*

Diamond anvil cell (DAC) experiments are static, with $P$ and $T$ determined through various calibrations, but cannot reach conditions resembling those in the deep Solar interior [34]. Shock experiments attain higher $T$ and $P$, but involve large uncertainties [44] and probe transient behavior, which is unlike the slowly evolving Sun. Atomic bomb detonations, which fuse deuterium

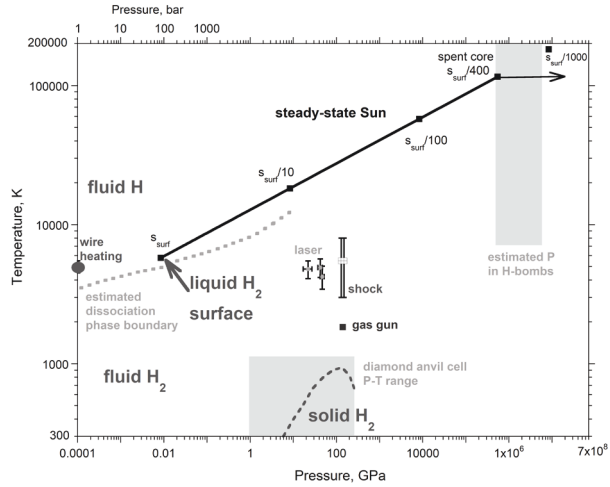


FIGURE 7
Calculated $T - P$ conditions in the Solar interior. Surface conditions (heavy arrow) are $P_{surf} =$ 85 bar from the ideal gas law and $T = 5775$ K from Table 2. Heavy black line = a least squares fit. Squares show possible sizes for cores, which are isothermal (e.g., thin arrow). Grey dotted curve = phase boundary estimated between fluid $H_2$ and H [44]. Big grey dot = complete dissociation at 1 bar [41]. Short grey rectangle shows $P - T$ space accessed in static diamond anvil cell experiments [34]. Dark gray symbols show various dynamic experiments on hydrogen [47, 48] and deuterium [49]. Long gray rectangle shows estimated conditions in bombs that convert deuterium and tritium to helium. A liquid solar surface is proposed (see text).

($D_2$) and/or tritium-rich fuels into helium, reach solar conditions (Figure 7) but are likewise transient. Conditions in bombs are modelled, as pressure standards and calibration are lacking [15]. Nonetheless, the range of pressures estimated for atomic bombs is consistent with our minimum core size, calculated from mass burning rates today (Section 3.2). Our spent core radius agrees with the minimum bomb pressure.

A larger core than that estimated from burning is expected due to density stratification of heavy elements in the Sun, much of which was inherited. A heavy metal core would constitute a dead central zone. If a minimum pressure is the sole requirement for fusion, then available shock experiments (Figure 7: [47–49]) suggest that an inert heavy metal core with $s_{surf}/100$ may exist.

### *3.4.2 Limits on fusion conditions*

From the minimum core size, our model indicates that solar fusion to He occurs where $P < 5 \times 10^5$ GPa and $T < 116{,}000$ K. A Sun that is compositionally stratified could have a larger heat producing radius. A very rough minimum is suggested by $s_{surf}/100$, see above. Thus, the lower limit for fusion is estimated as $P > 8300$ GPa and $T > 57{,}500$ K. Immense temperatures are not associated with fusion, but very high pressures are.

The above $T$ range is fairly narrow and well constrained. The $P$ range is wide and the minimum pressure is not well constrained. Further restricting the minimum $P$ requires additional information. Our best estimate is $\sim 10^5$ GPa ($10^9$ bars) from He production over time (Figure 7).

## 4 DISCUSSION

Our model is based on the stable thermal emissions of stars and their essentially spherical geometry, which together provide temperature vs radius with no free parameters. Assuming steady-state conditions and utilizing the model of Fourier and law of Stephan-Boltzmann shows that interior temperatures can only be high inside volumetrically insignificant cores (Figure 4). We show the increase in temperature with depth is dwarfed by the mounting pressures that stem from Newton's law of gravitation (Figure 6).

How robust is our model? Below, Section 4.1 shows that our model is consistent with well-established high-$T$ and high-$P$ behavior of matter. Section 4.2 revisits the assumptions, showing that our model is more general than is immediately apparent. Section 4.3 explains that only conditions in the inert core are significantly affected by the limitations of our model. Section 4.4 discusses model validation via long-standing empirical power laws. Implications of our findings are manifold (Section 4.5) because assuming LTE in complex numerical models such as the SSM has circumvented previous attempts to incorporate the flow of heat. Hence, interior profiles like those of the classical static model, which describes non-luminous stars, have held sway for over 100 years.

### 4.1 Our model depicts high temperature behavior regardless of stellar chemical composition

*4.1.1 Realistic thermal transport properties result from our model*

Calculated $\kappa$ for diffusive radiative transfer inside a greybody goes as $T^3$ only if spectral functions of the material are independent of both frequency and $T$ [50]. Matter is variably transparent and so should not follow the $T^3$ rule.

Star interiors are considered to be opaque with electrons moving independently of the cations. This plasmoidic state resembles metals, in which their outermost (conduction) electrons roam among the positive cations, whose nuclei are shielded from one another by the valance electrons. Measurements show that $\kappa$ linearly depends on $T$ for many metals, including in the molten state: examples are given in [20] (chapter 9). Thermal conductivity linearly depending on $T$ is a consequence of radiative diffusion of moderate frequency light inside a material, as shown both experimentally [51] and theoretically [20, 21, 51] for metals, semi-conductors, and insulators above some minimum temperature, typically $\sim$1000 K for non-metals. That the mechanism is diffusion of radiation (in the infrared region for laboratory

studies) is corroborated by how thermal conductivity depends on pressure and length-scale [20, 21].

Our results describe heat transport in a thermally stable star. That the microscopic mechanism is diffusion of radiation is consistent with their hallmark characteristic of luminosity, our assumptions, and the thermal response of diverse materials. Chemical composition being irrelevant is a consequence of steady-state radiative diffusion in spherical symmetry.

*4.1.2 Our temperature profile embodies Wien's law and Planck's curve*
Emissions from blackbodies and greybodies are described by a unique temperature which is inversely proportional to the peak wavelength (Wien's law):

$$\lambda_{peak} = \frac{b}{T} \qquad \text{or} \qquad \nu_{peak} \propto T \tag{32}$$

where $b = 2897.8\ \mu\text{m K}^{-1}$ is an experimentally determined constant. Wien's law can be obtained from the Planck curve [52] which is used to describe stars. Continuous spectral measurements of the Sun provide confirmation (see tables in [53]).

From the RHS of Equation (32), the temperature representing the surface of a luminous star is proportional to an energy ($h\nu_{\text{peak}}$). The peak frequency is proportional to the average $\nu$ [54], so $T$ in (32) is a statistical measure, and is connected with heat-energy but not identical, as espoused in countless thermodynamic books. The ideal gas EoS resting on contained energy (14) is a consequence of the Virial theorem and the gassy state [19]. The proportionality of this energy with temperature, although previously explained in terms of the kinetic theory of gas, is more general, since all matter emits heat-energy in accord with the blackbody curve and the material's spectral properties [32].

### 4.2 Assumptions and generality of the model

As widely accepted, stellar interiors are hydrostatic. Using the Stefan-Boltzmann law is likewise accepted. Fourier's model is indisputable. A few more remarks on the EoS are warranted:

- Temperatures in our model are determined independent of any EoS, as a consequence of energy conservation.
- Thus, the EoS only pertains to density and pressure. But, the proportionality constants for the ideal gas EoS are irrelevant, and do not bear on the predicted surface density. Surface pressure is constrained by the mass of the atmosphere, which is not part of the model. We estimated $P_{\text{surf}}$ using the ideal gas law, which result (85 bars) is roughly compatible with phase boundaries of [44].
- Conservation of energy during steady-state requires that inelastic losses during particle interactions such as collisions are offset by heat production.

Under steady-state, softness of atoms is irrelevant, and so is delocalization of the electrons from the nuclei.

Generality of our model, including its EoS, holds because the latter is based on conservation laws and the stringent requirements of a bound state. These principles are independent, as in the Virial theorem for a bound state, which is derived without using any conservation laws [19].

The combination of Equation (21), (24), and our $T(s)$ formula (7), is restrictive indeed. Yet, this combination simultaneously makes our model general.

### 4.3 Limitations of the model are "buried" in the stellar cores

Finite atom size is important, as this limits compression and drives phase transitions that reduce volumes, as is copiously documented at laboratory conditions [34]. Finite atomic size is not quantitatively addressed in our model, yet underlies the presence of a core. Various core sizes are considered, due to scant information on the Sun's interior.

### 4.4 Empirical power laws for main sequence stars are an outcome of our model

Our model is validated by its straightforward prediction of empirical luminosity-mass power law, $L \propto M^{3.3}$ for stars near solar mass [1]. The other empirical power laws for stars follow (Section 2.5). Different rules inferred previously for small ($M < 0.43$ solar) and huge stars ($M > 55$ solar) could also be consistent with our model because surface densities of very tiny and very large stars need not have the same surface density of 233 kg m$^{-3}$ deduced here for the Sun.

From basic descriptions of the interaction of light and matter [32] the visually imaged solar surface is a phase boundary. Dependence of this phase boundary on pressure and temperature, as expected from many thermostatic studies and as commonly observed, would produce different densities for the surfaces of very small and very large stars. The flat phase boundary of Figure 7, estimated by Mahon et al. [44], is consistent with the wide mass range being described by (29).

### 4.5 Implications of our steady-state model for stars

Temperatures in stellar interiors are high. Yet, except for point-mass cores, interior $T$ is only modestly higher than surface temperatures (Figures 4 and 5). Hence, compression dominates interior changes (Figures 6 and 7). The large gravitational field created by the immense mass of stars is undeniably important to their interiors, yet to date has played a secondary role in models, since the focus starting with Emden's [9] model has been on perceived enormous temperatures of heat-retaining, non-luminous objects, whose heat content rests on Kelvin's overturned hypothesis for the origin of starlight.

*4.5.1 Can convection occur?*

The linear $T$ dependence of our effective $\kappa$ is either weaker than or compatible with properties of diverse materials, including spectroscopic descriptions of high $T$, high frequency, radiative diffusion [20, 50]. Thus, the thermal gradient during steady-state can be carried by heat diffusion in the star, and convective motion of matter is not needed.

This finding is under scored by our steady-state gradient being much lower than Emden's adiabats. Convection is unexpected, except for the surface boundary layer where more rapid changes in $T$ are likely. Granularity indicates convection in this region of rapidly changing $T$, where the heat generated inside the star is lost to space. However, surface conditions are poorly constrained because $H_2$ cannot be detected spectroscopically and experiments at relevant high $P$ and $T$ on hydrogen are exceedingly difficult. Further discussion of the solar atmosphere or photosphere is beyond the scope of this report.

*4.5.2 Importance of high pressure to the Sun's interior*

As pressures increase, materials increasingly resist compression, approaching constant density: this is evident in measurements and in the popular forms used for the EoS of solids [36]. Temperature being elevated cannot obliterate the effect of extreme compression. When matter reaches an incompressible state, and if the atoms in crystalline solid can rearrange to provide a denser configuration, a phase transition occurs, reducing stored elastic energy. For example, diatomic solids convert from the rock salt to cesium chloride structure during compression. Gas and liquids lack long-range order, so crystallographic rearrangements are not relevant. Disorder is expected even at the surface temperatures, so rearranging is not germane to stellar interiors for another reason. Below we describe a possible volume-reducing reaction inside stars.

Few data exist regarding stellar interiors because light is received only from the thin outer $\sim$500 km photosphere and granulated surface. Sections 3.3.1 to 3.3.3 propose that the atmosphere is dissociated H, while the underlying photosphere is gradational, such that the granulated solar surface it rests on is some dense, liquid phase of $H_2$. However, we cannot rule out subsurface H since temperatures are increasing. Regarding the deeper interior, the relevant region in $P$, $T$ space of hydrogen is unexplored (Figure 7), so a mixture that includes both H and $H_2$ is possible, but is immaterial, as follows: Electron localization functions from molecular dynamics calculations demonstrate that even in the metallic state, electrons are strongly associated with the ions [55]. This finding recapitulates Pauli's principle of local charge neutrality, which has been amply confirmed through crystallographic measurements. Association of nuclei and electrons promotes electron capture, as follows:

*4.5.3 A macroscopic depiction of nuclear fusion promoted by compression*
Fusion involves a sudden reduction in volume on an atomic scale, and release of heat. Consequently, the probability of fusion is promoted by high pressure, and impeded by high temperature, in accord with LeChatelier's principle.

During steady-state, fusion proceeds only as fast as the heat evolved is lost. We envision that the reaction occurs as a front at some radius, which grows very slowly with time, leaving the denser He product lying below the reactants. A series of nuclear reactions is expected.

High temperatures upon formation cannot be required because young stars have very high spin [56]. The amount of kinetic energy is immense and closely matches the change in gravitational potential upon formation [19]. The available gravitational energy cannot simultaneously produce rapid spin and huge amounts of heat.

That pressure is key is obvious from comparing non-dimensional versions of Equations (7) and (25), repeated here for emphasis:

$$\frac{P(s)}{P_{surf}} = \left(\frac{s_{surf}}{s}\right)^3 \quad \text{vs.} \quad \frac{T(s)}{T_{surf}} = \left(\frac{s_{surf}}{s}\right)^{1/2} \tag{33}$$

Laboratory studies have shown that electron capture by $^7$Be is promoted by pressure [57]. This finding has been confirmed in experiments at low $T$ and on the effect of coordinating cations and on low-$T$ contraction, where rates are enhanced when the distance is reduced between the electron and nucleus (reviewed by [58]). Compression enhancing electron capture is supported by many theoretical investigations, most recently [59]. Because no evidence yet exists for any other nuclear process being influenced by compression, and such is unexpected, we propose that electron capture is the key, exothermic step during conversion of H to He. Construction of a new mechanism for fusion inside stars, with comparison to existing models, will be presented elsewhere.

## 5 CONCLUSIONS

Local or complete thermal equilibrium underlies previous models of stellar interiors. This approach cannot address the hallmark characteristic of main sequence stars: copious thermal emissions at an essentially constant low rate over enormous spans of time. In addition, the historical model, upon which subsequent work is based, was constructed (1) prior to statements of the 0$^{th}$ and 3$^{rd}$ laws; (2) prior to the recognition that stellar heat was generated by fusion reactions, not by gravitational contractions; and (3) without considering heat transfer. These shortcomings, especially applying an adiabatic equation-of-state throughout an object which has an internal heat

source, are fundamental and cannot be remediated through addendums and/or multiple free-parameters. Because subsequent approaches to stellar interiors have not addressed the original shortcomings, and include additional flaws (Section 1), models to date still consider stellar interiors to be unfathomably hot. Extreme temperatures are conventionally viewed as necessary for nuclear fusion, yet this very condition impedes the progress of exothermic reactions (LeChatelier's principle).

A much different picture of stellar interiors results from our parameter-free, analytical model which is based on steady-state flow of heat in hydrostatic, internally heated, stable stars. Heat internally produced in stars is manifest in their luminosity, and controls their interior temperature independent of all other factors. Crucially, the law of Stefan-Boltzmann, when combined with Fourier's definition of flux in spherical symmetry, requires that temperatures inside nearly spherical stars are inversely proportional to the square-root of radial distance above the region of heat production, and constant in the cores below.

Section 4 documents internal consistency and generality of our model. Dependence of $L$ on $M$ to the 3⅓ power is a direct outcome our model. Our simple derivation of the accepted empirical mass-luminosity power law validates our model and further points to control of main-sequence star surfaces by a phase boundary. The absence of free parameters and few assumptions make our model robust and parsimonious. Previous models of stellar interiors use many lumped parameters, which can mask incorrect physics [60], and numerical methods, where the actual steps taken may be hidden in computational algorithms.

Heat differs fundamentally from matter because any amount of energy can co-exist in a given volume. Matter resists compression but not infinitely. Hence, the immense pressure inside stars promotes fusion, analogous to phase transitions explored in the laboratory. High temperatures are the consequence of this exothermic reaction, not the cause.

## ACKNOWLEDGMENTS

This research was partially supported by National Science Foundation, grant number EAR-2122296.

## REFERENCES

[1] Zombeck, M. V. 2007 *Handbook of Space Astronomy and Astrophysics*. Cambridge: Cambridge Univ. Press; 2007, pp. 105–109, https://doi.org/10.1017/CBO9780511536359
[2] Roxburgh, I. W. *Solar Physics*, **100** (1985), 21, https://doi.org/10.1007/BF00158420
[3] Bahcall, J. N. *Neutrino Astrophysics*. Cambridge: Cambridge University Press; 1989.
[4] Kippenhahn, R.m Weigert, A. *Stellar Structure and Evolution*. Berlin: Springer-Verlag; 1990, https://doi.org/10.1007/978-3-642-30304-3

[5] Hansen, C. J., Kawaler, S. D., Trimble, V. *Stellar Interiors*. Berlin: Springer-Verlag, 2004, http://dx.doi.org/10.1007/978-1-4419-9110-2
[6] Prialnik, D. *An Introduction to the Theory of Stellar Structure and Evolution*. Cambridge, UK: Cambridge University Press, 2009.
[7] Maciel, W. J. *Introduction to Stellar Structure*. Cham: Springer-Verlag; 2016, http://dx.doi.org/10.1007/978-3-319-16142-6
[8] Mullen, D. J. *Physics of the Sun*, *2nd Ed*. Boca Raton: Taylor and Francis Group; 2023, ISBN 9780367710392.
[9] Emden, R. *Gaskuglen – Anwendungen de Mechanischen Wärmetheorie*. Leipzig: B. G. Teubner; 1907.
[10] Turck-Chièze, S., Cahen, S., Casse, S., Doom, M. *Astrophys. J*., **335** (1988), 415, https://doi.org/10.1086/166936
[11] Knauth, L. P. *Palaeogeogr. Palaeoclimatol. Palaeoecol*., **219** (2005), 53, https://doi.org/10.1016/B978-0-444-52019-7.50007-3
[12] Robert, F., Chaussido, M. *Nature*, **443** (2006), 969, https://doi.org/10.1038/nature05239
[13] Scotese, C. R., Song, H., Mills, B. J. W., van der Meer, D. G. *Earth Sci. Rev.*, **215** (2021), paper 103503, https://doi.org/10.1016/j.earscirev.2021.103503
[14] Lang, K. R. *Astrophysical Data: Planets and Stars*. New York: Springer-Verlag; 1992, http://dx.doi.org/10.1007/978-1-4684-0640-5
[15] https://en.wikipedia.org/wiki/Thermonuclear_weapon viewed 2023-02-18
[16] Phillips, A. C. *The Physics of Stars*. New York: John Wiley and Sons; 1999, ISBN 978-0-471-98798-7.
[17] Eddington, A. S. *The Internal Consitution of the Stars*. New York: Dover Publications; 1959.
[18] Pippard, A. B. *The Elements of Classical Thermodynamics*. London: Cambridge University Press; 1974.
[19] Hofmeister, A. M., Criss, R. E. *Can. J. Phys.*, **94** (2016), 380, https://doi.org/10.1139/cjp-2015-0468
[20] Hofmeister, A. M. *Measurements, Mechanisms, and Models of Heat Transport*. Amsterdam: Elesevier; 2019, https://doi.org/10.1016/C2015-0-06204-9
[21] Hofmeister, A. M. *Materials*, **14** (2021), Paper 449, https://doi.org/10.3390/ma14020449
[22] Zemansky, M. W., Dittman, R. H. *Heat and Thermodynamics, 6th ed*. New York: McGraw-Hill; 1981.
[23] Siegel, R., Howell, J. R. *Thermal Radiation Heat Transfer*. New York: McGraw-Hill; 1972.
[24] Brewster, M. Q. *Thermal Radiative Transfer and Properties*. New York: John Wiley and Sons; 1992.
[25] Blumm, J., Henderson, J. B., Nilson, O., Fricke, J. (1997). *High Temp.- High Pres.* **34** (1997), 555.
[26] Nusselt, W. *Gesundheits-Ingenieur*, **38** (1915), 477, 490, 872 (cited in Martin, H. Chem. Ing. Tech., **80** (2008), 1313. https://onlinelibrary.wiley.com/doi/pdf/10.1002/cite.200750748)
[27] Triton, D. J. *Physical Fluid Dynamics*. New York: Van Nostrand Reinhold Co.; 1977, http://dx.doi.org/10.1007/978-94-009-9992-3
[28] Lavenda, B. H. *Thermodynamics of Irreversible Processes*. New York: Halsted (Wiley); 1978, http://dx.doi.org/10.1007/978-1-349-03254-9
[29] Hofmeister, A. M., Criss, E. M., Criss, R. E. *Materials*, **15** (2022), 2638; https://doi.org/10.3390/ma15072638
[30] Meyers, M. A., Chawla, K. K. *Mechanical Behavior of Materials, 2nd ed*. Cambridge: Cambridge University Press; 2009. ISBN-13 978-0-521-86675-0
[31] Johnson, H. L. *Ann. Rev. Astron. Astrophys*., **4** (1966), 193, https://doi.org/10.1146/annurev.aa.04.090166.001205
[32] Bates, J. B. *Fourier Transform IR Spect*., **1** (1978), 99, http://dx.doi.org/10.1016/B978-0-12-254101-8.50008-3
[33] Maron, S. H., Prutton, C. F. *Principles of Physical Chemistry, 4th ed.* London: MacMillan; 1965.
[34] Mao, H. K., Chen, X. J, Ding, Y., Li, B. and Wang, L. *Rev. Modern Phys.*, **90** (2018), paper 0015007, https://doi.org/10.1103/RevModPhys.90.015007
[35] https://en.wikipedia.org/wiki/Mass%E2%80%93luminosity_relation viewed 2023-03-01

[36] Anderson, D. L. *New Theory of the Earth*. New York: Cambridge University Press; 2007, http://dx.doi.org/10.1017/CBO9781139167291
[37] Basu, S., Antia, H. M. *Phys. Repts*., **457** (2008), 217, https://doi.org/10.1016/j.physrep.2007.12.002
[38] https://apod.nasa.gov/apod/ap200203.html viewed 2023-02-10.
[39] Abhyankar, K. D. *Bull. Astron. Soc. India*, **5** (1977), 40–44.
[40] Züttel, A. (2004) *Naturwissenschaften*, **91** (2004). 157, http://dx.doi.org/10.1007/s00114-004-0516-x
[41] Langmuir, I. *J. Am. Chem. Soc*., **34** (1912), 860, http://dx.doi.org/10.1021/ja02208a003
[42] Jaeggli, S. A., Lin, H., Uitenbroek, H. *Astrophys. J*., **745** (2012), paper 133, http://dx.doi:10.1088/0004-637X/745/2/133
[43] Jansen, F., Chen, I., Machonkin, M. A. *J. Appl. Phys*., **66** (1989), 5749, https://doi.org/10.1063/1.343643
[44] McMahon, J. M., Morales, M. A., Pierleoni, C., Ceperley, D. M. *Rev. Mod. Phys*., **84** (2012), 1607, https://doi.org/10.1103/RevModPhys.84.1607
[45] Ouellette, R. J., Rawn, D. J. *Organic Chemistry*. Amsterdam: Elesevier, (ch. 1); 2014, https://doi.org/10.1016/C2013-0-14256-0
[46] Tanaka, H. *J. Chem. Phys.*, **153** (2020), Paper 130901, https://doi.org/10.1063/5.0021045
[47] Nellis, W. J., Weir, S. T., Mitchell, C. T. *Science* **273** (1996), 936, https://www.science.org/doi/10.1126/science.273.5277.936
[48] Loubeyre, P., Celliers, P. M., Hicks, D. G., Henry, E., Dewaele, A., Pasley, J., Eggert, J., Koenig, M., et al. *High Pressure Res.*, **24** (2004), 25, https://doi.org/10.1080/08957950310001635792
[49] Fortov, V. E., Ilkaev, R. I., Arinin, V. A., Burtzev, V. V., Golubev, V. A., Iosilevskiy, I. L., Khrustalev, V. V., Mikhailov, A. L., Mochalov, M. A., Ternovoi, V. Y. and Zhernokletov, M. V. *Phys Rev Lett.*, **99** (2007), paper 185001, https://doi.org/10.1103/PhysRevLett.99.185001
[50] Hofmeister, A. M. *Geophys. Res. Lett*., **41** (2014), 3074, https://doi.org/10.1002/2014GL059833
[51] Hofmeister, A. M., Dong, J. J., Branlund, J. M. *J. Appl. Phys*., **115** (2014) paper 163517 https://doi.org/10.1063/1.4873295
[52] Marr, J. M., Wilkin, F. P. *Am. J. Phys*., **80** (2012), 339, https://doi.org/10.1119/1.3696974
[53] Allen, C. W. *Astrophysical Quantities*. London: Athlone Press; 1973.
[54] Williams, B. W. *J. Chem. Educ*., **91** (2014), 623, https://doi.org/10.1021/ed400827f
[55] Geng, H. Y., Wu, Q., Marquez, M., Ackland, G. J. Phys. Rev. B, **100** (2019), paper 134109, https://doi.org/10.1103/PhysRevB.100.134109
[56] Dufton, P. L., Dunstall, P. R., Evans, C. J., Brott, I., Cantiello, M., De Koter, A., de Mink, S., Fraser, M., Hénault-Brunet, V., Howarth, I. D. et al. *Astrophys. J*., **743** (2011), L22, https://doi.org/10.1088/2041-8205/743/1/L22
[57] Hensley, W. K., Bassett, W. A., Huizenga, J. R. *Science*, **181** (1973), 1164, https://doi.org/10.1126/science.181.4105.1164
[58] Tkalya, E. V., Avdeenkov, A. V., Bibikov, A. V., Bodrenko, I. V., Nikolaev, A. V. *Phys. Rev. C*, **86** (2012), paper 014608, https://doi.org/10.1103/PhysRevC.86.014608
[59] Ray, A., Sikdar, A. K., Das, P., Pathak, S., Datta, *J. Phys. Rev. C*, **101** (2020), paper 035801, https://doi.org/10.1103/PhysRevC.101.035801
[60] Transtrum, M. K., Machta, B. B., Brown, K. S., Daniels, B. C., Myers, C. R., Sethna, J. P. *J. Chem. Phys.*, **143** (2015), paper 010901, https://doi.org/10.1063/1.4923066